Re-entrant spin glass and Magnetoresistance in $Co_{0.2}Zn_{0.8}Fe_{1.6}Ti_{0.4}O_4$ spinel oxide

R. N. Bhowmik* and R. Ranganathan

Experimental condensed Matter Physics Division,

Saha Institute of Nuclear physics,

1/AF, Bidhannagar, Calcutta 700064, India

Abstract

We have investigated the static and dynamical response of magnetic clusters in $Co_{0.2}Zn_{0.8}Fe_{1.6}Ti_{0.4}O_4$ spinel oxide, where a sequence of magnetic phase transitions, *i.e*, paramagnetic(PM) to ferromagnetic (FM) state at $T_C \leq 270$K and ferromagnetic to canted spin glass (CSG) state at $T_f \leq 125$K is observed. The time dependence of remanent magnetization shows a non-equilibrium spin dynamics in the CSG state and above 130K an weak time dependent relaxation characterizes a canted ferromagnetic state which is followed up by no relaxation effect in the paramagnetic state. The field dependence of the magnetization confirms the absence of long range ferromagnetic order in the system. This brings the idea that all the spins are not necessarily be infinite ordered inside the clusters due to spin canting effects. The variation of the ferromagnetic and antiferromagnetic components and magnetic disorder inside the clusters shows some interesting magnetic and electrical properties in the system, *viz*, field induced transition in M vs H data, re-entrant magnetic transition in ac susceptiblity vs T data and re-entrant semi-conducting behaviour in resistivity vs T data.

*e-mail address:rnb@cmp.saha.ernet.in

I. INTRODUCTION

Recently, extensive research activities are going on a variety of colossal magneto resistance (CMR) materials, which includes substituted manganite $R_{1-x}A_xMnO_3$ [R= trivalent rare earth ion, A= divalent alkaline rare earth ion] [1] and spinel ferrites such as $Fe_{1-x}T_xCrS_4$ [T=Cu,Zn etc.] [2,3] and $Co_xMn_{3-y}O_4$ [4]. The substitution by magnetic or non-magnetic ions has shown a tremendous effect in controlling the magnetic and electrical properties of a magnetic materials. As for example, the parent manganite $LaMnO_3$ is an antiferromagnet and insulator. But the substituted manganites show ferromagnetism with metallic behaviour below the Curie temperature T_C [1]. The competition between ferromagnetic (metallic) and antiferromagnetic (insulator) exchange interactions change the the polaronic hopping between $Mn^{4+}(t_{2g}^3e_g)$-O-$Mn^{3+}(t_{2g}^3e_g^1)$ in substituted manganites [5]. Besides the polaronic hopping, it has also been suggested that double exchange mechanism via Mn^{3+}-O-Mn^{4+} ions, Jahn-Teller distortions due to Mn^{3+} ions and strong electron-phonon coupling are contributing to CMR effect in perovskites materials [1].

In general, there is no mixed valence Mn^{3+} - Mn^{4+} ions or double exchange mechanism in spinel ferrites. In spinel lattices, the anions (O^{2-}, S^{2-} ions) form a cubic close packing, in which the interstices are occupied by tetrahedral (form A sites or sublattice) and octahedral (form B sites or sublattice) coordinated cations, gives rise the formula unit AB_2X_4 (A represent A site cations, B represent B site cations, X represent anions). The competition between ferromagnetic and antiferromagnetic superexchange interactions occurs between the spins of inter-sublattices and intra-sublattices as A-O-B (J_{AB} = inter-sublattice exchange interaction), B-O-B (J_{BB} = B site intra-sublattice interaction) and A-O-A (J_{AA} = A site intra-exchange interaction). In collinear spinel structure $|J_{AB}| >> |J_{BB}| >> |J_{AA}|$ and the system shows long range ferrimagnetic (ferromagnetic) order [6]. If A sublattice magnetic dilution is below the percolation limit ($C_A \approx$ 0.33 -0.4), the J_{AB} and J_{BB} will be comparable and magnetic frustration appears in the B sublattice. Then B site spins form finite size clusters. The spins inside the clusters may be canted due to short range antiferromagnetic

interactions of nearest-neighbours. The longitudinal components (S_z) of a canted spin will contribute long range ferromagnetic ordering along the broken axis of symmetry (z axis) whereas the transverse components S_t will contribute spin glass ordering in x-y plane [6]. The competition between ferromagnetic and antiferromagnetic interactions and magnetic disorder in B sites have shown spin glass or re-entrant spin glass behaviour in spinel oxides [7–9].

Recently, it has been observed that the existence of ferromagnetic clusters (magnetic polarons) with itinerent charges (charges are itinerant within the clusters) in either an antiferromagnetic insulating matrix or paramagnetic insulating matrix exhibits an unusual magnetic properties with large CMR effect [1,5]. It has been found theoretical by Aharoni et al. [10] and experimental by Hücker et al. [11] on $La_{2-x}Sr_xCu_{1-z}Zn_zO_4$ that charge compensating defects like magnetic ion vacancy can significantly modify the effective exchange interactions by renormalizing the concentration of frustrated bonds and hopping conductivity of a system. The frustrating bond will behave like a magnetic dipole, which makes the superexchange interactions more ferromagnetic inside the clusters. It has also been suggested [12] that the existence of different valence cations in B site can enhance the conductivity in spinel oxides. To test the effect of cation vacancy and existence of mixed valence cations like Fe^{2+}/Fe^{3+}, extensive studies have been performed in $Fe_{3-x}M_xO_4$ [M = Ti^{4+},Zn^{2+}] spinel oxides [13]. The results showed significant enhancement in conductivity with increasing cation vacancy and mixed valence cations in B sites.

In order to understand the magnetic ordering of B site clusters with intra spin canting, we have studied the $Co_{0.2}Zn_{0.8}Fe_2O_4$ spinel oxide [14]. We have considered that the magnetic clusters are randomly distributed in the antiferromagnetic B site matrix. In this presentation, we have replaced Fe^{3+} by non-magnetic Ti^{4+} in $Co_{0.2}Zn_{0.8}Fe_2O_4$ with the motivation to study the effects of Fe^{2+}/Fe^{3+} mixture, cation vacancies in B sites.

II. EXPERIMENTAL

A. Sample preparation and Characterization

We have prepared $Co_{0.2}Zn_{0.8}Fe_{1.6}Ti_{0.4}O_4$ solid solution by conventional solid state method. The stoichiometric amount of powder oxides of 99.5% Co_3O_4 (from Fluka), 99.998% Fe_2O_3 (from Johnson Matthey), 99.998% ZnO (from Johnson Matthey) and 99.995% TiO_2 (from Johnson Matthey) have been mixed and grinded for $\approx$ 2 hours. The mixture have been pelletized under the pressure of 9 tons/cm^2 and heated at 950^{0}C for 12 hours and at 1200^{0}C for 24 hours. The system has been finally sintered at 1400^{0}C for 24 hours with intermediate grinding and pelletizing. Through out process the heating and cooling rate was maintained at 3^{0}C/minute and 2^{0}C/minute, respectively. Room temperature X-ray diffraction spectrum has beeen taken using Philips PW1710 diffractometer with Cu K_α radiation. The XRD spectrum (Fig.1a) shows a well crystalline cubic spinel structure with lattice parameter (a) $\approx$ 8.4184 $\mathring{A}$.

The room temperature Mössbauer spectrum (Fig.1b) in absence of magnetic field has been recorded in transmission geometry using a 25 mCi ^{57}Co source in Rh matrix. The paramagnetic spectrum consists of two Lorentzian doublets arising from B site Fe^{3+} ions and Fe^{2+} ions respectively and a Lorentzian singlet due to A site Fe^{3+} ions. The fitted values of isomer shift (IS) and quadrupole splitting (QS) are +0.098 mm/sec, +0.339 mm/sec for B site Fe^{3+} and +0.808 mm/sec, 0.760 mm/sec for B site Fe^{2+} ions respectively. The IS value for the A site Fe^{3+} ion is -0.181 mm/sec. The IS and QS values are calculated with respect to Fe metal and with $\pm$0.002 mm/sec error. The values are in good agreement previously reported for ferrites [8,15]. The most probable cation distribution (with error =$\pm$ 0.001) obtained using standard least square method is $(Zn^{2+}_{0.8}Fe^{3+}_{0.047}Ti^{4+}_{0.153})_A[Co^{2+}_{0.2}Fe^{3+}_{1.530-\delta}Fe^{2+}_{0.023}Ti^{4+}_{0.247}]_BO_4$ (A: tetrahedral sites, B: octahedral sites). The term δ represent the cations vacancy to maintain the charge neutrality in B site [13] or if δ is 0, then there is a possibility to obtain T^{4+} and Ti^{3+} mixtures in B sites [12].

B. Measurements

The low field ac susceptibility in the temperature range 60K to 325K with ac field ~ 1 Oe and frequency range 37 Hz to 7.7 kHz and dc magnetization data under zero field cooled (ZFC) and field cooled (FC) condition have been recorded using home made magnetometer [16]. For FC condition the cooling field and the measurement field was maintained at the same value. The time dependence of remanent magnetization have been observed by field cooled condition with waiting time (t_w) $\approx$ 300 seconds. High field magnetic measurements have been performed using SQUID magnetometer. The dc resistivity as a function of temperature in absence and presence of magnetic field has been measured by two probe method using Kethley 6517A high resistance electrometer and Kethley 2001 multimeter has been used for magnetoresistance measurement at T$\sim$ 240K to 315K.

III. RESULTS

A. AC susceptibility

The real (χ') and imaginary (χ'') components of ac susceptibility (Fig.2) show the following features ,*i.e.*, a small maximum at $T_p \approx$ 240K, a plateau like behaviour in the temperature range : $125 < T > 240$K, low temperature maximum at $T_f \approx$ 125K, the decrease of ac susceptibility above T_p and below T_f. These are the good characteristics for re-entrant magnetic phase transitions in a magnetic system [17]. The rounded maximum in χ', χ'' vs T at T_p suggest that the magnetic clusters of different size, instead of individual spins, are showing magnetic response at T_p. Further, the absence of any significant shift of T_p (Fig. 2) in the frequency range 37 Hz to 7.7 kHz of 1 Oe ac field suggests a strong ferromagnetic interactions inside the clusters [18]. If there was no cluster size distribution, T_p should have been represented the curie temperature T_C of the system. However, keeping in mind the cluster size distribution, it is expected that magnetic response of the largest clusters will occur at $T > T_p$. In this case, it is not proper to call T_p as the Curie temperature T_C, where

the system undergoes a paramagnetic to ferromagnetic state on decreasing the temperature. Therefore, the Curie temperature of the system is defined as the inflection point of χ' at T_C $\approx$ 270K and the difference between T_C and T_p ($\sim$ 30K) is due to the existence of various size cluster below T_C [19]. If the magnetic clusters are assumed as the ferromagnetic domains, the absence of strong divergence in ac susceptibility data below T_C suggest that the clusters in this system do not represent long range ordered ferromagnetic domains below T_C. However, the plateau like behaviour in χ', χ'' vs T data below 240K suggest the ferromagnetic ordering of the clusters [17] with the spin-spin correlation length (l) restricted to less than the size of the clusters due to various factors like spin canting, random occupation of the magnetic and non-magnetic moments inside the clusters. The plateau like behaviour may also be affected by the demagnetising field in the very thin semi-disc (length >> breadth) shaped sample. However, the qualitative features of the sample will not signicantly changed due to the demagnetizing field effects. The effect of demagnetising field becomes less important and is expected to be almost independent of sample shape in this system, as the cluster size is smaller than the percolation limit where large number of spins are infinite long range ferromagnetic ordered [20].

Focussing on the low temperature maximum in χ' and χ'' (Fig. 2), it is observed that T_f ($\approx$ 125K) shows a significant frequency shift (marked by arrow). This signals the appearance of more frustrated magnetic state with spin glass character at low temperature. The T_f(f) were estimated by first order derivative of χ' with rest to temperature and the data (with $\pm$ 2% accuracy) were fitted with Vogel-Fulcher law

$$f = f_0 exp^{-E_a/(T_f - T_0)} \tag{1}$$

The ln(f) vs $1/(T_f - T_0)$ data are shown in Fig.2b inset. The fitted parameters are $f_0 \approx 10^7$ Hz, $E_a \approx$ 220K and $T_0 \approx$ 106K. These parameters suggest the freezing of clusters below T_f. This justify to define T_f is as cluster spin freezing temperature for this system. The spin glass feature at $T \leq T_f$ suggest that short range antiferromagnetic interaction is becoming significant as $T \rightarrow T_f$ from high temperature side and competing with ferromagnetic inter-

actions which is observed below 240K. The sharp decrease of χ' and χ'' suggest the increase of spin canting inside the clusters on lowering the temperature [17,20]. As a consequence domain wall motion of the clusters is hindered below T_f due to random anisotropy field [21].

B. DC magnetization

Fig.3a shows the zero field cooled (ZFC) and field cooled (FC) dc susceptibility (M/H) with magnetic field H = 10 Oe to 85 Oe and temperature range T = 20K to 320K. If the temperature continues to decrease, the ZFC susceptibility shows a broad maximum at $T_f \approx$ 125K. Below T_f, the ZFC susceptibility decreases upto our lowest measurement temperature 20K. The ZFC susceptibility is almost dc fields independent below 70K, as observed in other re-entrant system where low temperature regime shows spin glass behaviour but strong field dependent ferromagnetic regime appear as the temperature increases [22]. The inverse of zero field cooled susceptibility (χ_{dc}^{ZFC}) vs T plot above 275K shows an upward curvature and the data above 295K fit with (Fig.3a inset) Curie-Weiss law

$$\chi_{dc} = \frac{C}{T - \theta_w} \tag{2}$$

The fitted parameters are Curie constant (C) ≈ 0.144 emu-K/g/Oe and the asymptotic Curie temperature (θ_w) $\approx +$ 270K. The intercept of the inverse ZFC susceptibility on the positive temperature axis suggest a dominant ferromagnetic interactions in this system below $T_C \approx$ 270K.

The FC susceptibility shows an weak magnetic irreversibility at T_{irr} ($< T_C$), which is followed by FC susceptibility maximum close to T_f with strong magnetic irreversibility at low temperature (see Fig.3a inset for 10 Oe FC and ZFC data). The decrease of FC susceptibility below T_f can be attributed due to the strong antiferromagnetic interactions or due to the local random anisotropy below below T_f [17]. Fig.3b inset shows that irreversibility temperature T_{irr} and cluster spin freezing temperature T_f decreases with increasing magnetic field. The appearance of an weak magnetic irreversibility below T_C and strong magnetic irreversibility below T_f suggest the re-entrant magnetic behaviour [17] in this system.

C. Magnetic hysteresis

We have shown magnetic field (H) dependence of ZFC isothermal magnetization (M) in Fig.4. The system shows some remarkable feature in M vs H plot. The 10K data show an S shape at low field regime, while the 30K and 60K data show a field induced magnetic transition at $H_{cf} \sim 1$ Tesla and 1.5 Tesla, respectively. It is also observed that after 4 quadrant field cycling ($0 \rightleftharpoons H_{max}$ and $0 \rightleftharpoons H_{min}$), the field induced transition occurs at higher fields, *i.e.*, $H_{cf} \sim 1.7$ Tesla and 3 Tesla for 30K (Fig.4b) and 60K, respectively. The 100K do not show any field induced transition at + H axis but small field induced transition is observed at ≈ -1 Tesla. At T ≥ 150K no field induced transitions are observed. Similar phase induced transitions have been observed in a variety of disordered magnetic materials where the materials segregates into two distinguishable electronic states that coexist within the same crystallographic phase [5,17,23–26]. The most reasonable explanation for such type of field induced transition is that the system undergoes an antiferromagnetic to metastable ferromagnetic state at $H > H_{cf}$. This is further confirmed that there is no long range ferromagnetic order in the system, rather the antiferromagnetic interactions promotes strong spin canting inside the clusters below 100K and the ferromagnetic state above T_f (≈ 125K) is very similar to canted ferromagnets [17,26]. The same features are observed in the M vs H plots where magnetization shows lacks of saturation even upto 8 Tesla. The low value of coercive field above 125K and no magnetic hysteresis above 150K suggest ferromagnetic regime of the sample. However, the rapid increase of coercive field below 100K (Fig.5 inset right scale) definitely suggest the blocking of domain wall motion in the spin canting state [17,21].

By inspecting the positive slope of H/M vs M^2 at T ≤ 250K, we assumed that the paramagnetic to ferromagnetic phase transition in this system is second order [25,27]. We have calculated the spontaneous magnetization (M_S) using modified Arrot plot (Fig.5)

$$M^{1/\beta}(H) \propto (H/M)^{1/\gamma} \tag{3}$$

A self consistent method to obtain the best fitted parameters was considered [27]. In this procedure, first we have estimated the values of critical parameters using 250K data and modified Arrot plots were constructed using this parameters for all the temperatures. The linear extrapolation of high field magnetization data to $M^{1/\beta}$ axis gives the M_S value and the linear extrapolation to $(H/M)^{1/\gamma}$ axis gives the inverse of initial susceptibility. The M_S values were applied to the equation: M_S (T) $\propto$ (T_C - T)$^{1/\beta}$ for T $< T_C$. The modified Arrot plots were reconstructed using the obtained values of β. Finally, we obtained the best fitted values as : $\beta = 1.03 \pm 0.02$, $\gamma = 0.70 \pm 0.01$ and $T_C \approx 265$K $\pm$2K. The exponent values are close to that reported values for Heisenberg ferromagnets with strong magnetic disorder [28]. The temperature dependence of the M_S (Fig.5 inset left scale) suggest that M_S value at 10K ($\sim$ 46 emu/g) is less than the values obtained at 30K and 60K ($\sim$ 53 emu/g). This is due to the spin canting effect at low temperature.

D. Time and temperature dependence of dc magnetization

We have investigated the time dependence of field cooled remanent magnetization for better understanding of competition between equilibrium and non-equilibrium dynamics in the system. The experimental data (point symbol) in Fig.6a show a clear and systematic change of time dependent curvature from concave down (at T $\leq$ 130K) to concave up as the measurement temperature increases. We have found that the remanent magnetization decay at low temperature regime (T $\leq$ 130K) is best fitted by the superposition of a pure stretched exponential and a constant term as

$$M_R(t) = M_0 + M_1 exp^{-(t/\tau)^n} \tag{4}$$

where M_0, M_1, τ and n are fitted parameters (shown in Table 1). The M_0 parameter represents intrinsic ferromagnetic contribution and M_1 relates to a glassy component at the measurement temperature [18]. Above, 130K the remanent magnetization decay is not well fitted by equation (3). However, the best fit of 142K data require the product of a power law term with the stretched exponential function as

$$M_R(t) = M_0 + M_1 t^{-\alpha} exp^{-(t/\tau)^n} \quad (5)$$

where M_0, M_1, α, τ and n are the fitted parameters (shown in Table 1). In general, the power law decay of remanent magnetization has been considered as a weak time dependent function and represents an equilibrium spin dynamics of a ferromagnetic system [29], where as the stretched exponential function represent the non-equilibrium slow spin glass dynamics [22]. The relaxation of the system above the cluster spin freezing temperature $T_f \approx 125$K suggest that it is not in a true ferromagnetic state. The disorder and frustration in the ferromagnetic state takes into account the two competitive times scale simultaneously, one is due to intra-cluster dynamics [18] and second one is due to the cluster growth in presence of the frustration [30]. According to a model proposed by Chamberlin and Haines [31] that relaxation rate (ω_s) of a cluster with size 's' is related as

$$\omega_s \sim exp(C/s) \quad (6)$$

where C is a constant. This equation suggest that as the cluster size decreases, the relaxation rate will be faster. This is possible as the thermal activated process, on increasing temperature, will decrease the cluster size. In the temperature range T$\geq$ 166K to 251K, the time dependence of remanent magnetization follows a power law, similar to that has been observed in a re-entrant ferromagnet [29] by the equation

$$M_R(t) = M_0 + M_1 t^{-\alpha} \quad (7)$$

with the fitted parameters shown in Table 1. It has been found that the remanent magnetization at 280K is practically independent of time ($M_R(t) \approx M_0$) and the small value of M_0 is due to the short range interacting clusters in the paramagnetic state [28].

The temperature dependence of the field cooled remanent magnetization (M_{TRM}), after removing the cooling field $\approx$ 60 Oe, is shown in Fig.6b. The data clearly show a change in the nature of remanent magnetization decay at a tempearure $T_S \approx 130$K. We have found that TRM data at T$\leq$ 130K decay as

$$M_{TRM} \propto exp(-\alpha T) \quad (8)$$

where as the TRM data at T $> 130K$ follow a simple power law decay as

$$M_{TRM} \propto T^{-\beta} \tag{9}$$

The implication of the above two equations is that the thermal activated process slowly reduces the glassy behaviour exhibits below T_S in comparison with the fast decay in the ferromagnetic state. However, the non-zero value of M_{TRM} at 280K is consistent with our assumption that it is due to the short range interacting clusters in the paramagnetic state.

E. Temperature dependence of dc resistivity

As a complimentary support for the existence of re-entrant magnetic state, we have measured the resistivity (ρ) as a function of temperature and magnetic field. Fig.7a shows ρ vs T plot at zero and 7.8 kOe magnetic field. The zero field resistivity rapidly increases below 270K and shows slow increase below 200K that indicates the presence of ferromagnetic ordering below 200K. The high resistivity values even below 200K suggest that the ferromagnetic interaction is weak in this system [32]. The strong increase of resistivity below 100K suggest that antiferromagnetic interaction is dominating over the ferromagnetic one due to strong spin canting effect at low temperature. The resistivity follows an exponential function as $\rho \sim \exp^{E_g/kT}$ in both the regimes, suggests semi-conducting behaviour of the system. The fitted value of the activation energy (E_g) is decreasing from $\approx$ 0.239 eV (for T $> 200K$) to 5.98 meV (for T $<$ 200K). This informs that the paramagnetic like disordered state become more ordered (ferromagnetic) below 200K [33].

It is observed (Fig.7a) that as the temperature decreases below 320K, resistivity under field (ρ (7.8 kOe)) remains greater than ρ (0) value upto T$\approx$ 270K. Then ρ (7.8 kOe) $\sim$ ρ (0) upto 240K but increases upto $T_{SM} \approx$ 175K, where the system shows field induced semiconductor to metal transition. On further decreasing temperature, ρ (7.8 kOe) decreases before showing a sharp increase below the field induced metal to semiconductor transition at $T_{MS} \approx$ 80K. This is a re-entrant semi-conducting (S-M-S) behaviour [34] in our system. The

magnetoresistance (MR) calculated (from Fig.7a) using the formula $\Delta\rho/\rho_0[=(\rho_{7.8kOe}\text{-}\rho_0)/\rho_0]$ shows $\approx$ 80% (-ve) change at T_{MS}, $\approx$ 20% (-ve) at T_{SM}, $\approx$ 40% (-ve) at 200K and positive MR above 270K.

The comparison of resistivity (ρ (H)) with the ac susceptibility data (Fig.7a right scale) shows that the positive magnetoresistance occurs in the paramagnetic regime (T> $T_C\approx$ 270K), the negative MR is observed below T_p where the clusters show ferromagnetic ordering and the magnetoresistance again decreases in the spin glass regime (T < 100K). The difference between the ac susceptibility maximum at $T_p \approx$ 240K and the ρ (H) maximum at 175K probably due to the existence of different size clusters in the system. Depending on the size and random distribution of magnetic and non-magnetic ions inside the clusters, the proportion of ferromagnetic (metallic) and paramagnetic (semi-conducting) contributions will vary from cluster to cluster in the system. These clusters are called magnetic polarons or ferrons [34,5]. Some of the clusters, which are paramagnetic in nature, will show semi-conducting and most of the clusters, which are ferromagnetic in nature, will show metallic behaviour. As a result, instead of showing ρ (H) maximum near to T_p or T_C, the system shows ρ (H) maximum at $\approx$ 175K. This behavior is in contrast to the conventional CMR perovskites where ρ (H) occurs near to T_C [1]. The resistivity in presence of magnetic field, therefore, confirms that there is no long range ferromagnetic order in this system and the spin-spin correlation length varies from cluster to cluster. Below 175K, the high magnetic field strongly reduces the paramagnetic effect and increases the size of ferromagnetic clusters. As the spin-spin correlation length increases in presence of field, the scattering of the charge carrier decreases and the enhancement of the electron hopping inside the clusters show metallic behaviour in the system. The appearance of canted spin glass state at T $< T_f$, where antiferromagnetic interaction dominates, will the spin-spin correlation length and increases the electron scattering process inside the clusters. The localization of electrons in spin canted states show sharp increase of resistivity [5].

We have also measured the magnetoresistance (MR), after zero field cooling from 300K to the measurement temperature ($\sim$ 240K to 315K). The temperature has been kept constant

with maximum fluctuation ± 0.1K during the measurement period. We find (Fig.8) an appreciable change in magnetoresistance $\Delta\rho/\rho_0[=(\rho_H\text{-}\rho_0)/\rho_0]$ for magnetic field ± 7.8kG. It is to be noted (Fig.8a) that the MR is negative at 247K and suggests dominant ferromagnetic contribution. For T ≥ 252K, the MR initially shows positive value and then crossover to negative value as the applied field increases. This indicates a competition between ferromagnetic and paramagnetic response of the clusters below T_C. On further increasing the measurement temperature, the system shows positive MR (Fig.8b) at T ≥ T_C (≈ 270K) (Fig.8c) in the paramagnetic regime. The positive MR in the paramagnetic state may be due to the Lorentz force [35], which causes bending ('twisting') of the conduction electron's path, or grain boundary scattering as expected for polycrystalline sample in the paramagnetic state [1]. To confirm about the cross over from negative to positive MR near to Curie temperature (T_C), we have continued the MR measurement at a particular temperature for more than one field cycling(0 Oe → 7.8kOe → 0 Oe → -7.8 kOe → 0 Oe). Fig.9a shows that the MR at T = 252K ($< T_C$) continuously decreases on cycling the field for three times, in contrast to the continuously increasing trend (Fig.9c) at 289K ($> T_C$). However, if we look at the 272K (near to T_C) data (Fig.9b), the MR value never gets back to the starting point after the one cycle field application. The continuation of increasing or decreasing trend of magnetoresistance is related to relaxation [36] or memory effect [1,23] in the sample.

IV. DISCUSSION

The magnetic and complementary resistivity measurements of $Co_{0.2}Zn_{0.8}Fe_{1.6}Ti_{0.4}O_4$ spinel oxide give the signatures of re-entrant spin glass behaviour, eventhough, the existence of a true re-entrant spin glass phase is still a matter of debate for 3-dimensional system [22,37]. The experimental results will be discussed by assuming the existence of various size clusters. The ferromagnetic behaviour has been understood by treating these clusters as magnetic domains, inside of which all the spins are not necessarily be infinite long range ordered due to spin canting effects, random distribution of magnetic and non-

magnetic ions and different proportion of ferromagnetic and antiferromagnetic interactions inside the clusters. The temperature dependence of ac susceptibility data suggest that domain formation occurs above 240K. As the temperature decreases, canted spin structure is favoured inside the domains due to antiferromagnetic interactions. As a result, the random anisotropy field introduced by Dzyalosinsky-Moriya type interactions $\sim \vec{S_i} \mathrm{x} \vec{S_j}$ will hinder the (cluster) domain wall movement and decrease the low field ac susceptibility at low temperature [17]. The frequency dependence of ac susceptibility (χ', χ''), the weak irreversibility (between FC and ZFC susceptibility) below T_C ($\approx$ 270K) and strong irreversibility below T_f ($\approx$ 125K) give the characteristic feature of typical re-entrant ferromagnet [29]. The re-entrant character of the system is further confirmed by the time dependence of the field cooled remanent magnetization experiments. The slow spin dynamics at T$\leq$ 130K suggest the non-equilibrium canted spin glass state, where as an equilibrium spin dynamics is dominating over the non-equilibrium dynamics in the ferromagnetic phase (weak time dependent) and the spin dynamics, then, approaches toward a time independent disordered (paramagnetic) phase as observed at 280K. The relaxation data along with field dependence of magnetization data also confirm that there is no long range ferromagnetic order, rather the system is a canted ferromagnet.

The most attractive feature of the present system is that the magnetic ordering and transport properties are highly correlated. The Mössbauer analysis suggests the existence of Fe^{3+} and Fe^{2+} ions and charge compensating defects (due to valence mismatch between Ti^{4+} and Fe^{3+} ions) like cation vacancies in B site [13]. The charge compensating defects can give rise ferromagnetic interactions by renormalizing the concentration of frustrated bonds [10]. Simultaneously, the charge fluctuations among the cations (Ti^{4+}/Fe^{2+} to Ti^{3+}/Fe^{3+}) in B site clusters will enhance the electron (polaron) hoping mechanism [12] and consequently the system shows large electrical conductivity. On the otherhand, tetravalent non-magnetic Ti^{4+} ions substitution in place of magnetic Fe^{3+} ions makes the inter-sublattice interactions Fe_B^{3+}-O^{2-}-Fe_A^{3+} almost negligible and the magnetic interactions depends on the B site superexchange interactions like Fe_B^{3+}-O^{2-}-Fe_B^{2+}, Fe_B^{3+}-O^{2-}-Ti_B^{3+}, Fe_B^{2+}-O^{2-}-Ti_B^{4+} etc. From

the various measurements, it is observed that although there exists both ferromagnetic and antiferromagnetic superexchange interactions, the dominant one is the ferromagnetic interactions which is observed from the intercept of the inverse of susceptibility on positive temperature axis. The appearance of metallic like resistivity behavour in presence of dc field at 80K to 175K range strongly suggest that magnetic exchange interactions are also affecting the electrical properties of the sample.

V. CONCLUSIONS

In conclusion, the present system $Co_{0.2}Zn_{0.8}Fe_{1.6}Ti_{0.4}O_4$ exhibits re-entrant magnetic phase transitions, *i.e.* paramagnetic to ferromagnetic state at $T_C \approx 270$K and ferromagnetic to canted spin glass state at $T_f \approx 125$K. The re-entrant behaviour in magnetic and in electrical resistivity data is attributed due to the cation vacancy and charge fluctuation effects inside the ferromagnetic clusters (magnetic polarons). The ferromagnetic state is not a typical long range ordered type, rather than a canted ferromagnetic one, where longitudinal spin components show ferromagnetic order and transverse spin components show spin glass order at low temperature. Without Neutron diffraction experiment, it is very difficult to say whether the ferromagnetic order of longitudinal spin components is still maintaining in canted spin glass state. However, the variation of exchange interactions, random distributions of cations from cluster to cluster may give rise inhomogeneity in electronic phase, *i.e.* a mixture of metallic (ferromagnetic) and semi-conducting (antiferromagnetic) components within the same cluster, eventhough, the system is in same crystallographic (cubic spinel) phase.

Acknowledgement: One of the authors RNB thanks to The Council of Scientific and Industrial Research (CSIR, New Delhi, India) for providing fellowship [F. No. 9/489(30)/98-EMR-I]. We also thank C. Bansal, S. sarkar and S. Kumar for helping in Mössbauer data support.

REFERENCES

[1] N. D. Mathur, G. Burnell, S. P. Isaac, T. J. Jackson, B. -S. Teo, J. L. MacManus-Driscoll, L. F. Cohen, J. E. Evetts and M. G. Blamire, Nature **387**, 266(1997)

[2] A. P. Ramirez, R. J. Cava and J. Krajewski, Nature **386**, 156(1997)

[3] S. Wang, Y. Sun, W. song, S. Ye, J. Dai, K. Li, J. Fang, X. Cao and Y. Zhang, J. Appl. Phys. **90**, 1407(2001)

[4] J. Philip and T. Kutty, Materials Letters **39**, 311(1999)

[5] R. Mahendiran, A. Maignan, C. Martin, M. Hervieu, and B. Raveau, Phys. Rev. B **62**, 11644(2000).

[6] J. L. Dormann, M. Nogues, J. Phys. C: Condens. Matter **2**, 1223(1990)

[7] D. Fiorani, S. Viticoli, J. L. Dorman, J. L. Tholence, A. P. Murani, Phys. Rev. B **30**, 2776(1984)

[8] R. A. Brand, H. Georges-Gibert, J. Hubsch and J. A. Heller, J. Phys. F: Met. Phys. **15**, 1987(1985)

[9] R. Sing and S. C. Bhargava, J. Phys: Condens. Matter **7**, 8183(1995)

[10] I. Ya. Korenblit, A. Aharony, and O. Entin-Wohlman, Phys. Rev. B **60**, R15017(1999)

[11] M. Hücker, V. Kataev, J. Pommer, J. Haraβ, A. Hosni, C. Pflitsch, R. Gross and B. Büchner, Phy. Rev. B **59**, R725(1999)

[12] W. Sugimoto, H. Yamamoto, Y. Sugahara and K. Kuroda, J. Phys. Chem. Solids **59**, 83(1998)

[13] N. Guigue-Millot, N. Keller and P. Perriat, Phys. Rev. B **64**, 012402 (2001)

[14] R. N. Bhowmik and R. Ranganathan, J. Magn. Magn. Mater. **248**, 101(2002)

[15] N.N. Greenwood, T.C. Gibb, Mössbauer Spectroscopy, (Chapman and Hall, London), 266(1971)

[16] A. Ray, A. Chakravarti, R. Ranganathan, Rev. Sci. Instrum., **67**, 789(1996); A. Chakravarti, R. Ranganathan and A. K. Raychaudhuri, Pramana-J. Phys. **36**, 231(1991)

[17] S. Mukherjee, R. Ranganathan and S.B. Roy, Phys. Rev. B **50**, 1084 (1994); S. Mukherjee, R. Ranganathan and S.B. Roy, Solid State Comm. **98**, 321 (1996)

[18] R. S. Freitas, L. Ghivelder, F. Damay, F. Dias and L. F. Cohen, Phys. Rev. B **64**, 144404 (2001)

[19] X. Liu, X. Xu and Y. Zhang, Phys. Rev. B **62**, 15112 (2000)

[20] B. V. B. Sarkissian, J. Phys. F: Metal Phys., **11**, 2191 (1981)

[21] I. A. Campbell and S. Senoussi, Phil. Mag. B **65**, 1267 (1992); I.A. Campbel, S. Senoussi, F. Varret, J. Teillet and A. Hamzic, Phys. Rev. Lett. **50**, 1615 (1983)

[22] K. Jonason, J. Mattsson and P. Nordblad, Phys. Rev. B **53**, 6507 (1996)

[23] I. Gordon, P. Wagner, V. V. Moshchalkov, Y. Bruynseraede, M. Apostu, R. Suryanarayanan and A. Revcolevschi, Phys. Rev. B **64**, 092408 (2001)

[24] H. Nojiri, K. Kaneko, M. Motokawa, K. Hirota, Y. Endoh and K. Takahashi, Phys. Rev. B **60**, 4142 (1999)

[25] D.A. Filippov, R.Z. Levitin, A.N. Vasil'ev, T.N. Voloshok, H. Kageyama and R. Suryanarayanan, Phys. Rev. B **65**, 100405 (2002)

[26] S. Radha, S.B. Roy, A.K. Nigam and G. Chandra, Phys. Rev. B **50**, 6866 (1994)

[27] J. Mira, J. Rivas, M. Vazquez, J.M. Garcia-Beneytez, J. Arcas, R.D. Sanchez and M.A. Senaris-Rodriguez, Phys. Rev. B **59**, 123 (1999)

[28] A. Belayachi, J. L. Dormann and M. Nogues, J. Phys.: Condens. Matter **10**, 1599 (1998)

[29] P. Mitchler, R. M. Roshko and W. Ruan, J. Appl. Phys. **73**(1993)

[30] D.N. Nam, K. Jonason, P. Nordblad, N.V. Khiem and N.X. Phuc, Phys. Rev. B **59**, 4189 (1999)

[31] R. V. Chamberlin and D. N. Haines, Phys. rev. Lett. **65**, 2197(1990)

[32] A. Maignan, A. Sundaresan, U.V. Varadaraju and B. Raveau, J. Magn. Magn. Mater. **184**, 83 (1998)

[33] M. A. Ahmed, and M. A. El Hiti, J. Phys. III **5**, 775(1995)

[34] M. A. Senaris-Rodriguez, J. B. Goodenough, J. Solid State Chem. **118**, 323(1995)

[35] K. P. Belov, Physics-Uspekhi **37**, 563(1994)

[36] M. A. Senaris-Rodriguez, M. P. Breizo, S. Castro, C. Rey, M. Sanchez, J. Mira, A. Fondado, J. Rivas, International Journal of Inorganic Materials **1**, 281(1999)

[37] T. Sato, T. Ando and T. Ogawa, Phys. Rev. B **64**, 184432 (2001)

Table 1: The fitted parameters M_0, M_1, n, τ and α of equations 4, 5 and 7 while fitted with time dependence of remanent magnetization data. For detais see text.

T(K)	M_0 $\pm\Delta$	M_1 $\pm\Delta$	n $\pm\Delta$	τ	$\alpha\pm\Delta$
80K	0.164±0.002	1.327±0.001	0.068±0.001	10^5 s	-
90K	0.260±0.001	0.728±0.001	0.227±0.001	10^5 s	-
109K	0.270±0.004	0.679±0.001	0.158±0.001	10^5 s	-
120K	0.373±0.003	0.390±0.002	0.219±0.001	10^5 s	-
130K	0.259±0.005	0.573±0.001	0.130±0.001	10^5 s	-
142K	0.272±0.002	0.511±0.001	0.090±0.001	10^5 s	0.006±0.0005
166K	0.463±0.003	0.228±0.001	-	-	0.115±0.0001
189K	0.283±0.003	0.069±0.001	-	-	0.276±0.0001
216K	0.150±0.002	0.063±0.001	-	-	0.118±0.0002
251K	0.109±0.001	0.015±0.001	-	-	0.194±0.0001
280K	-	-	-	-	-

Figure Caption

Fig.1a XRD data for $Co_{0.2}Zn_{0.8}Fe_{2-x}Ti_xO_4$ spinel oxide, b) Mössbauer spectrum recorded in absence of magnetic field at 300K. Solid point: experimental data, dotted/solid line is the fitted data using least square method

Fig.2 Temperature dependence of real (χ') and imaginary (χ'') component of ac susceptibility measured at 1 Oe ac field in the frequency range 337 Hz to 7.7 kHz. The inset Fig. shows the expt data fitted with Vogel-Fulcher law

Fig.3 a) Zero field cooled dc susceptibility vs temperature measured at different fields. The inset shows the zero field cooled (ZEC) and field cooled (FC) magnetization vs temperature measured (top corner) and Curie-weiss law fit to expt data (at close interval) measured at 10 Oe. b) field cooled dc susceptibility vs temperature and the cluster freezing temperature (T_f) and irreversible temperature (T_{irr}) at different fields.

Fig.4 Hysteresis loop shown for 10K to 300K. The solid line represents the increase of M as H increases 0 to 7 tesla. The open symbol shows the loop. The arrow up indicate the field where field induced transition ocurs. The horizontal arrow represent the M (axis) values at the temperature indicated. For details see in the text.

Fig.5 Modified Arrot plot ($M^{1/\beta}$ vs $(H/M)^{1/\gamma}$ with $\beta = 1.03$ and γ 0.7) for temperature 10K to 300K. The dotted line is the linear extrapolation of $M^{1/\beta}$ (for H> 3 Tesla) to H = 0 axis to calculate the spontaneous magnetization and the solid lines are drawn for guide to eye. Inset shows temperature dependence of spontaneous magnetization (M_S) and coercive field (H_C)(right scale).

Fig.6 a) Time dependence of remanent magnetization measured at different temperatures, b) Temperature dependence of remanent magnetization. T_S is the temperature which separate two decay regions.

Fig.7 a) Temperature dependence of resistivity at 0 Oe and 7.8 kOe and ac susceptibility at 1 Oe, 337 Hz (right scale). b) magnetoresistance calculated by subtracting 7.8 kOe data from 0 Oe data. For T_f, T_p, T_{MS} and T_{SM} see in the text.

Fig.8 Magnetoresistance measured at different temperatures with maximum field 8 kOe for

$Co_{0.2}Zn_{0.8}Fe_{2-x}Ti_xO_4$ spinel oxide.

Fig.9 Magnetoresistance measured for more than one cycle of applied field ± 8 kOe.

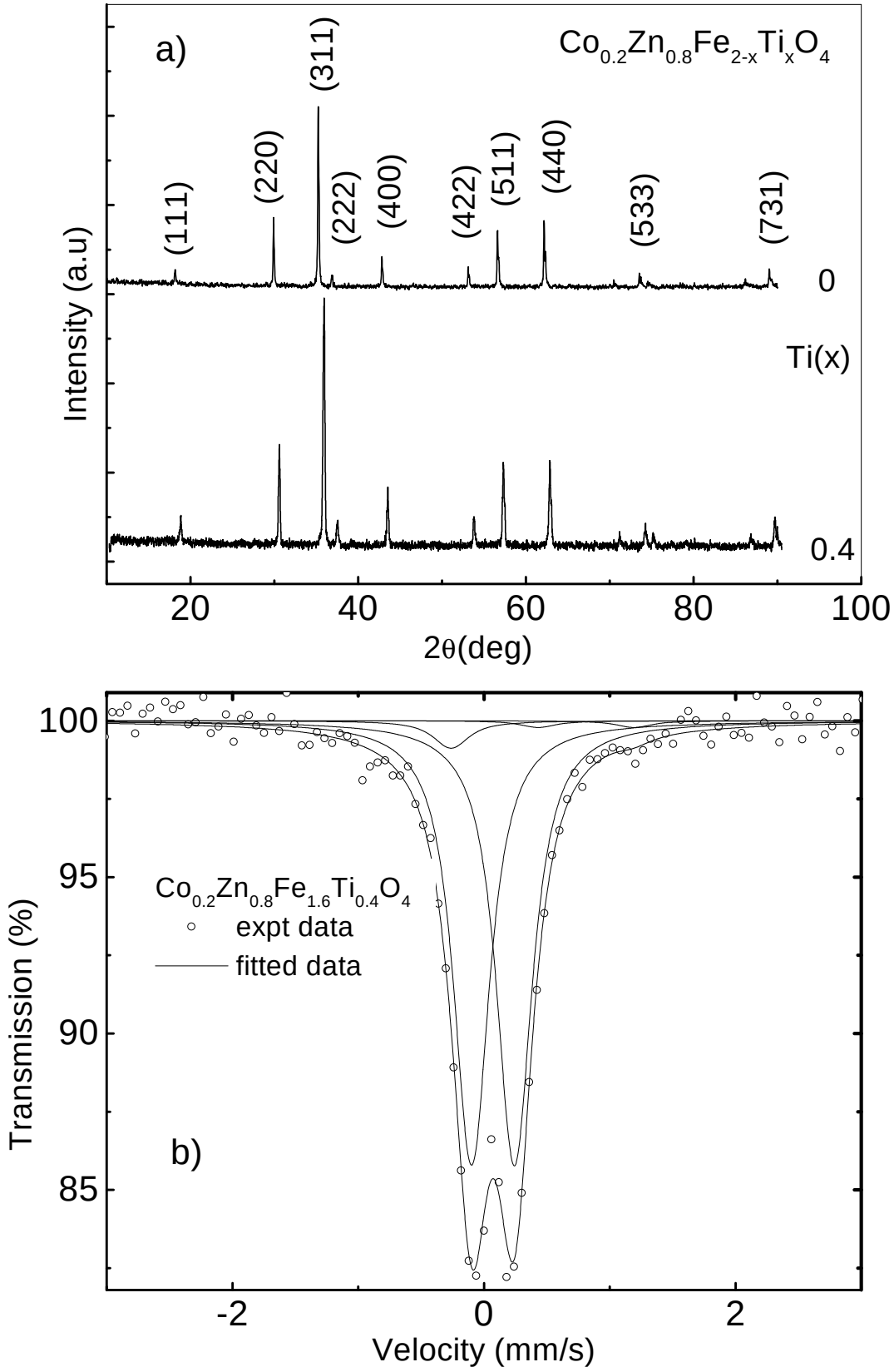

Fig.1 a) XRD data for $Co_{0.2}Zn_{0.8}Fe_{2-x}Ti_xO_4$ spinel oxide,
b) Mossbauer spectrum recorded in absence of magnetic field at 300K.
solid point: experimental data,
dotted/solid line is the fitted data using least square method.

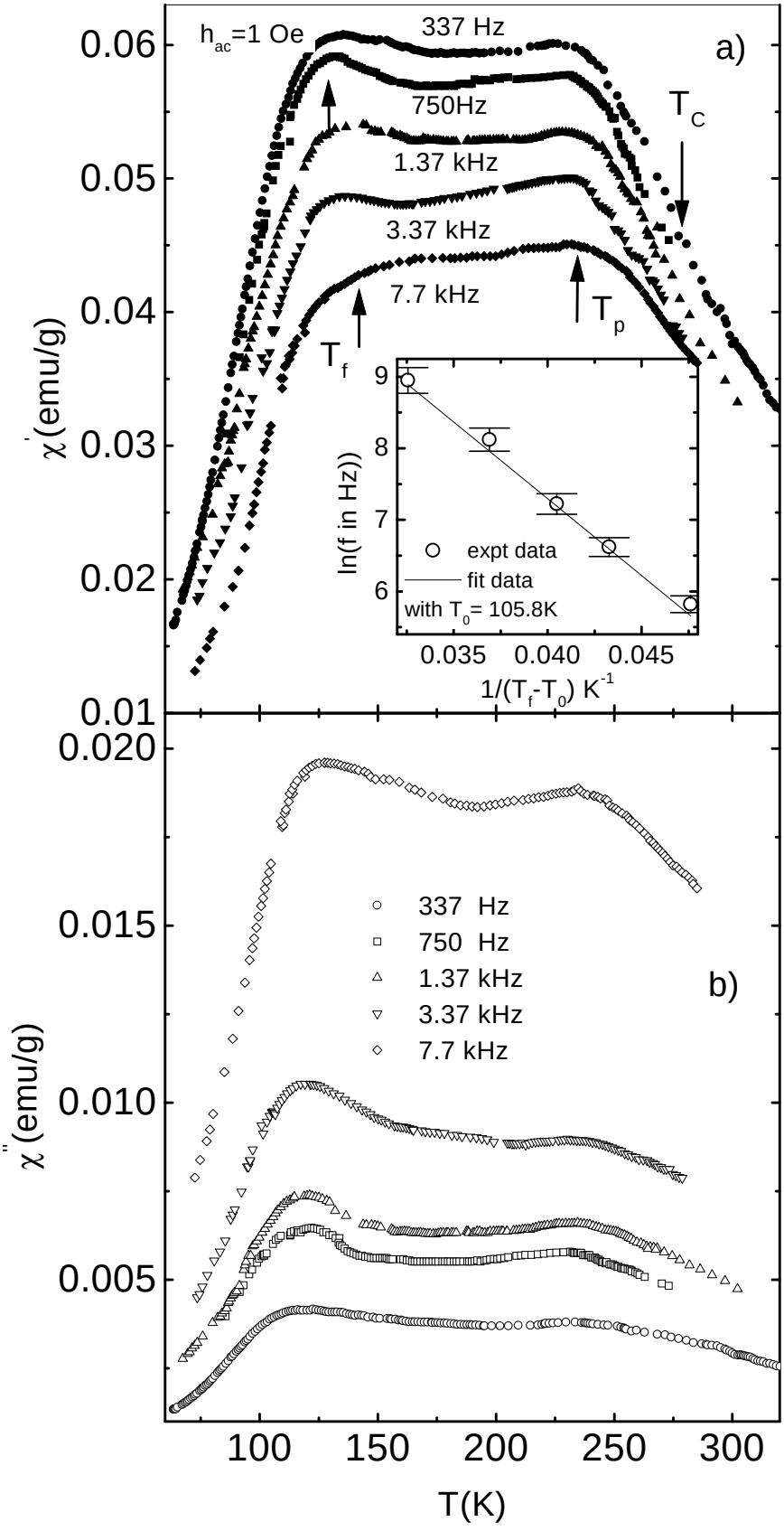

Fig.2 Temperature dependence of real(χ') and imaginary (χ'') component of ac susceptibility measured at 1 Oe ac field in the frequency range 337 Hz to 7.7 kHz. The inset Fig. shows the expt data fitted with Vogel-Fulcher law

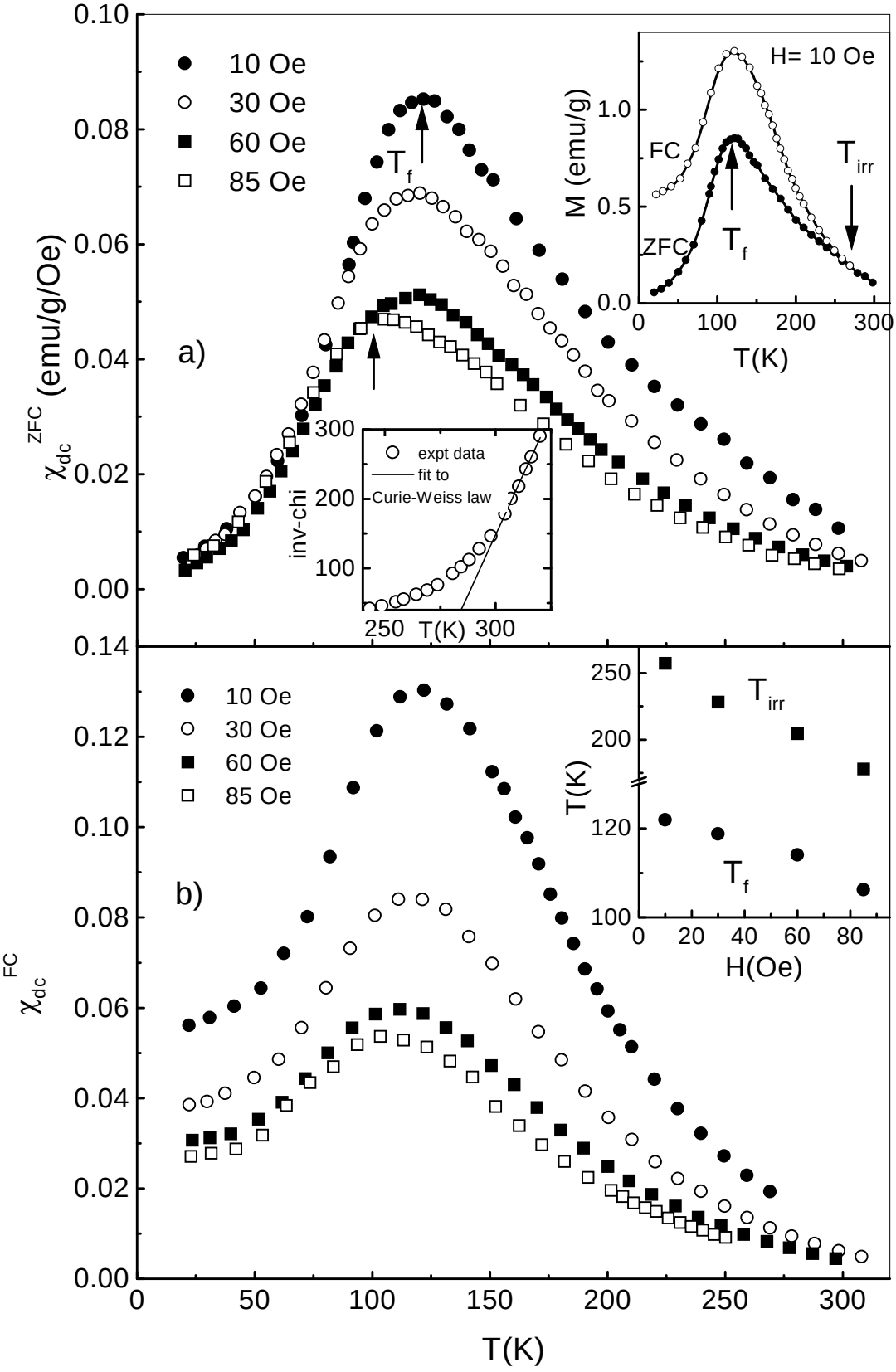

Fig.3 a) Zero field cooled dc susceptibility vs temperature measured at different fields. The inset shows the ZFC and FC magnetization vs temperature (top corner) and Curie-Weiss law fit to expt data (at close interval) measured at 10 Oe. b) field cooled dc susceptibility vs temperature and the cluster freezing temperature (T_f) and irreversible temperature (Tirr) at different fields.

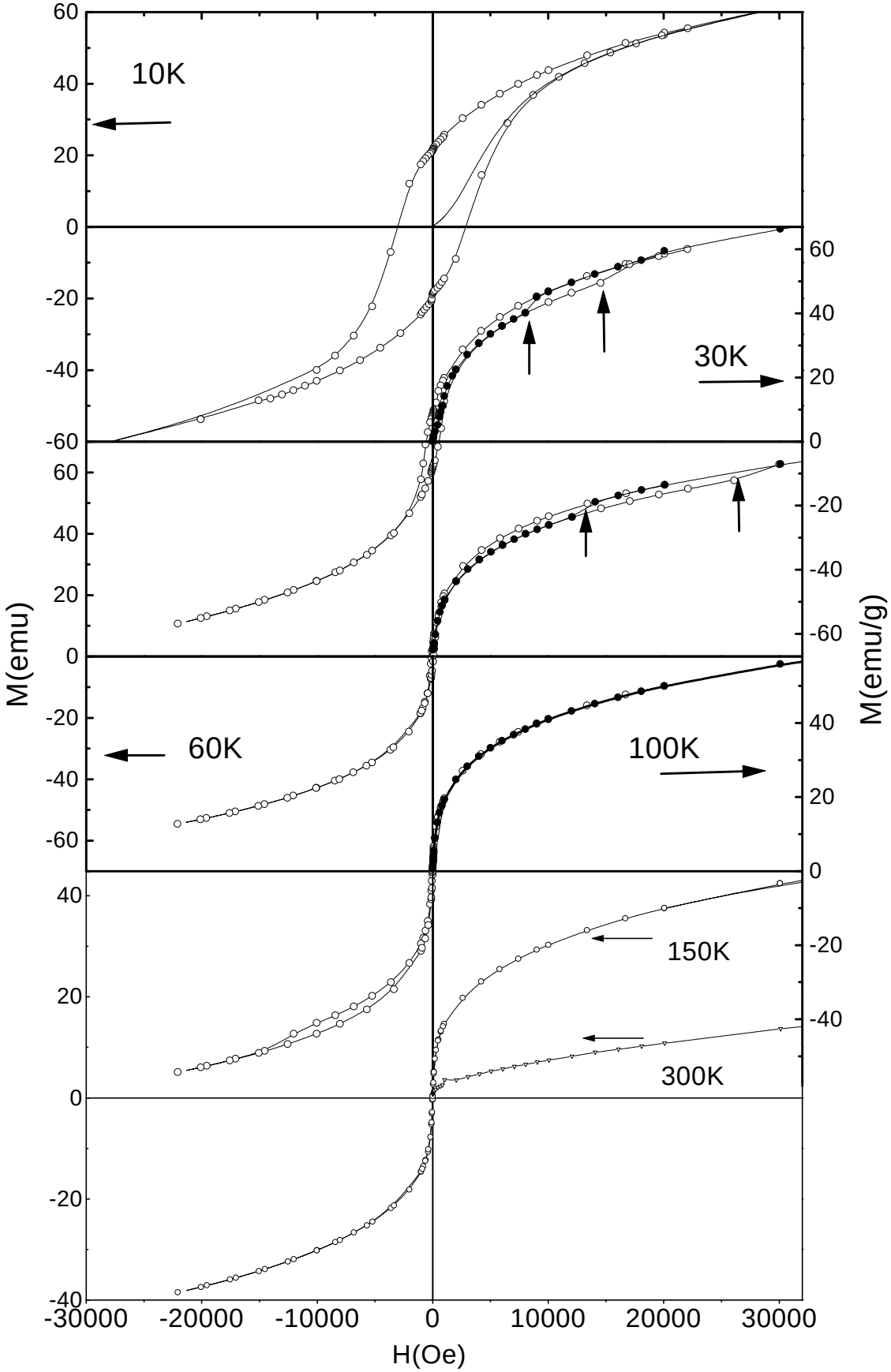

Fig.4 Hysteresis loop shown for 10K to 300K. The solid line represents the increase of M as H increases 0 to 7 Tesla. The open symbol shows the loop. The arrow up indicate the field where field induced transition occurs. The horizontalarrow represent the M (axis) values at the temperature indicated. For detail see in the text.

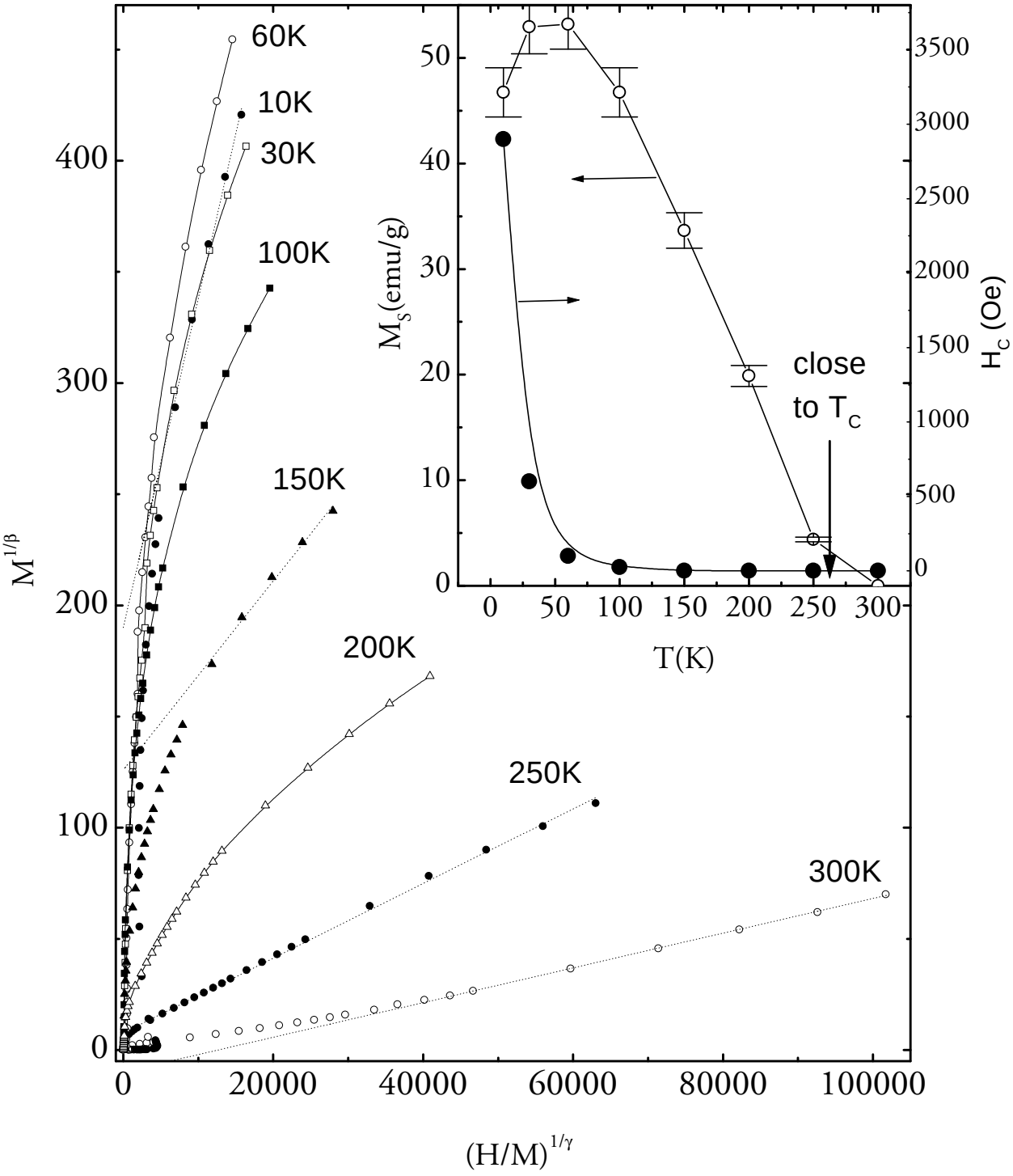

Fig.5 Modified Arrot plot ($M^{1/\beta}$ vs $(H/M)^{1/\gamma}$ with β=1.03 and γ= 0.7) for temperature 10K to 300K. The dotted line is the linear extrapolation of $M^{1/\beta}$ (for H >3 Tesla) to H = 0 axis to calculate the spontaneous magnetization and the solid lines are drawn for guide to eye. Inset shows temperature dependence of spontaneous magnetization (M_S) and coercive field (H_C) (right scale).

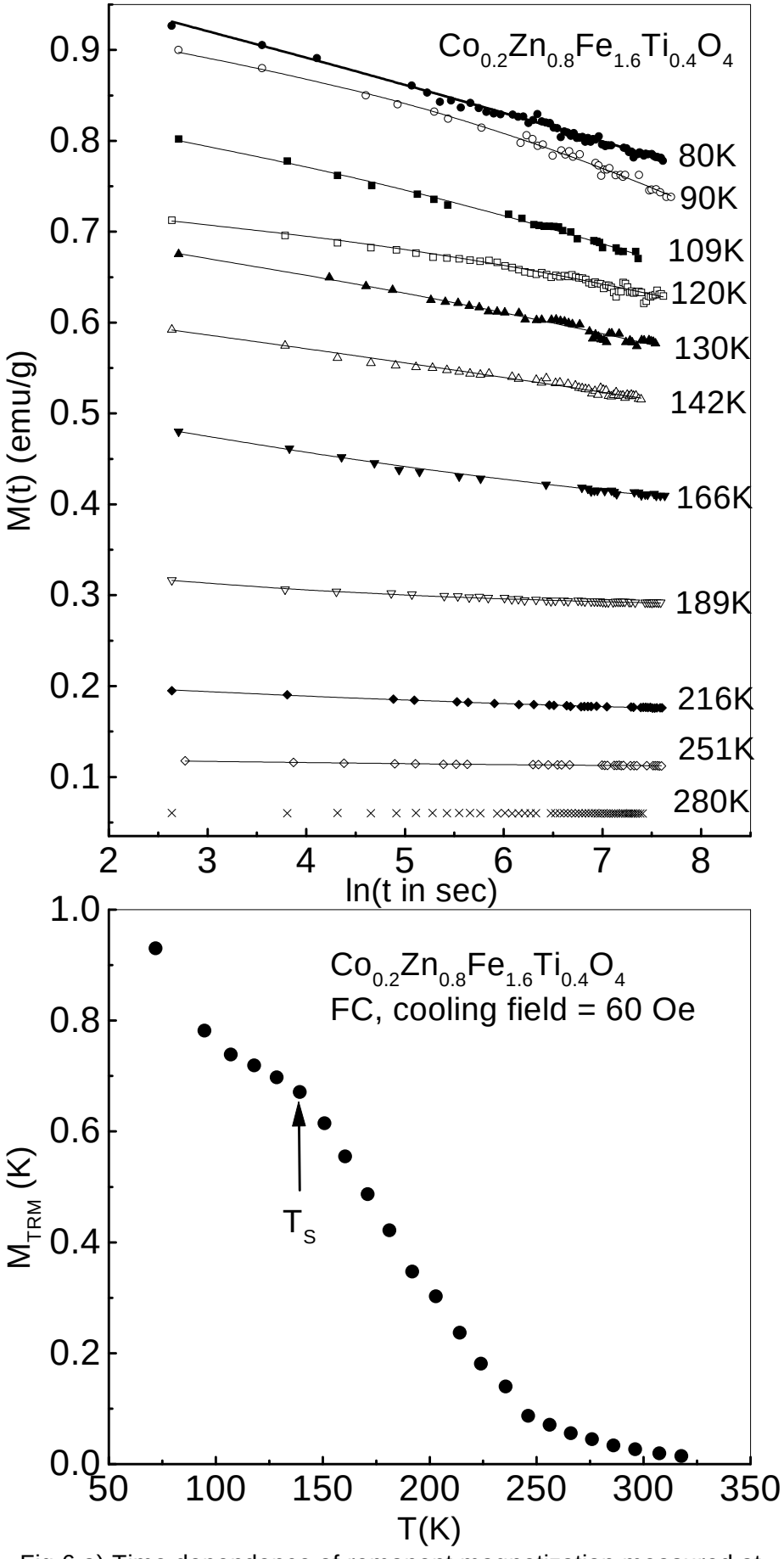

Fig.6 a) Time dependence of remanent magnetization measured at different temperatures, b) Temperature dependence of remanent magnetization. T_S is the temperature which separate two decay regions.

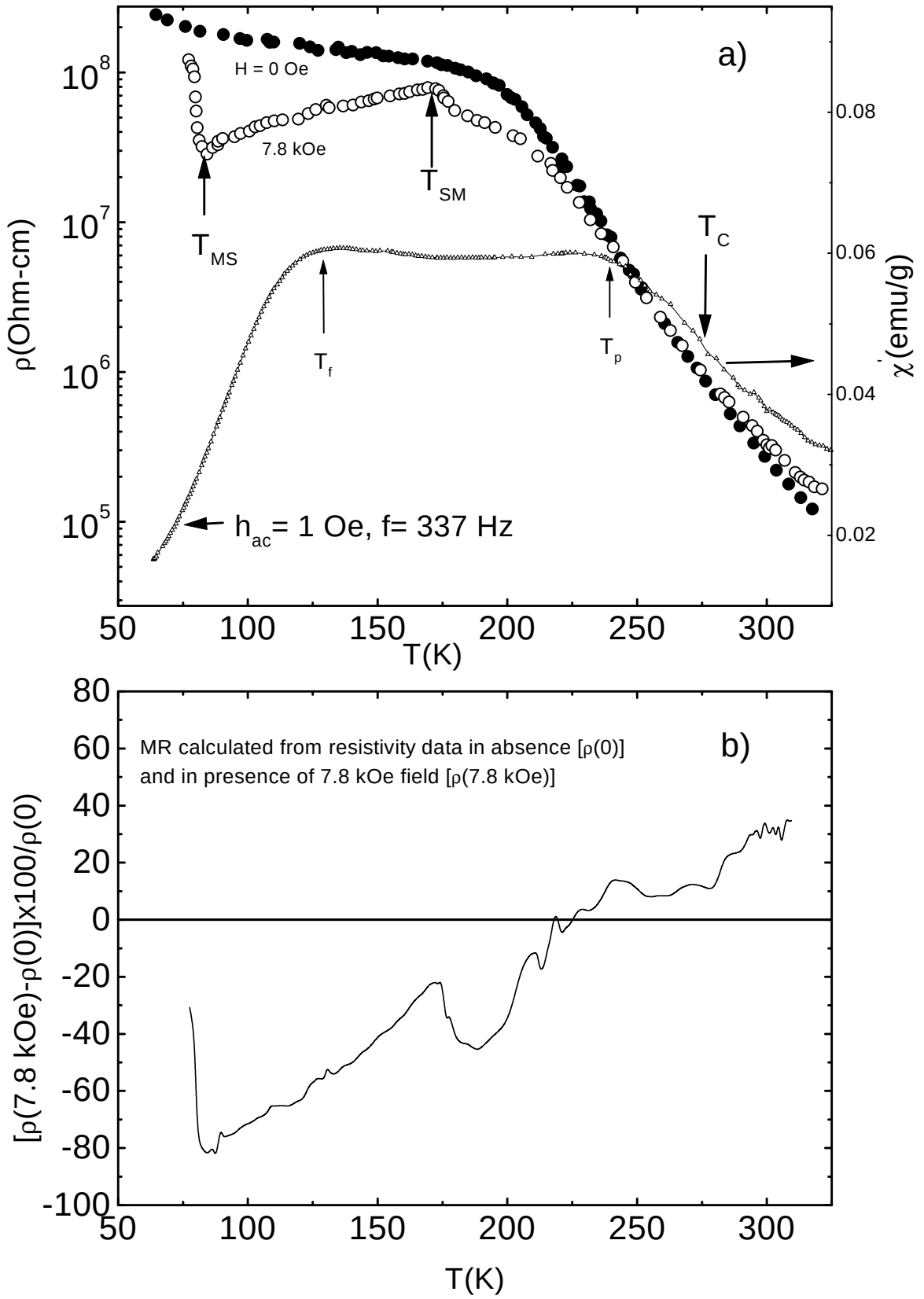

Fig.7 a) Temperature dependence of resistivity at 0 Oe and 7.8 kOe and ac susceptibility at 1 Oe, 337 Hz (right scale). b) magnetoresistance calculated by subtracting 7.8 kOe data from 0 Oe data. For T_f, T_p,T_{MS} and T_{SM} see in the text.

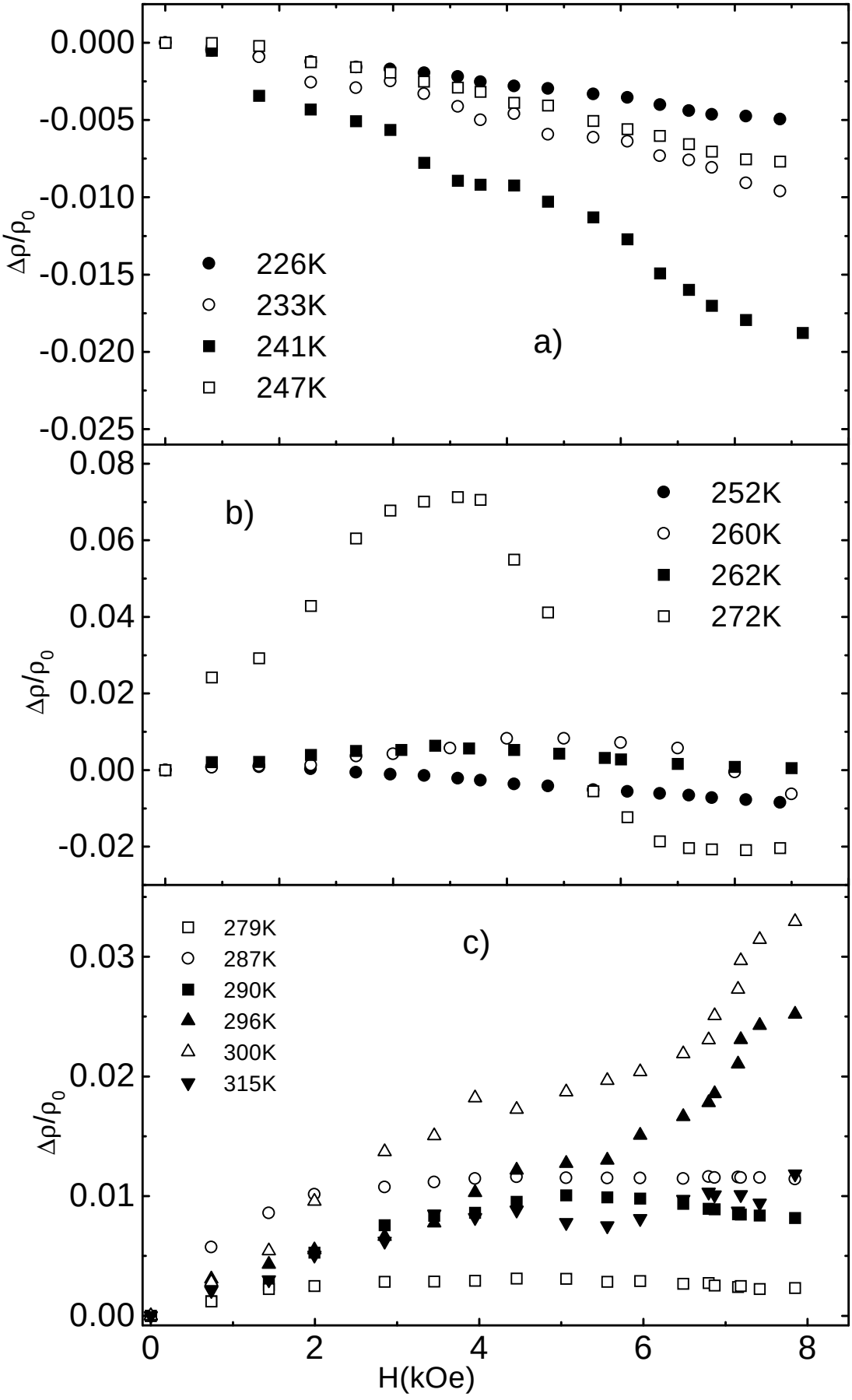

Fig.8 Magnetoresistance measured at different temperatures with maximum field 8 kOe for $Co_{0.2}Zn_{0.8}Fe_{1.6}Ti_4O_4$ spinel oxide.

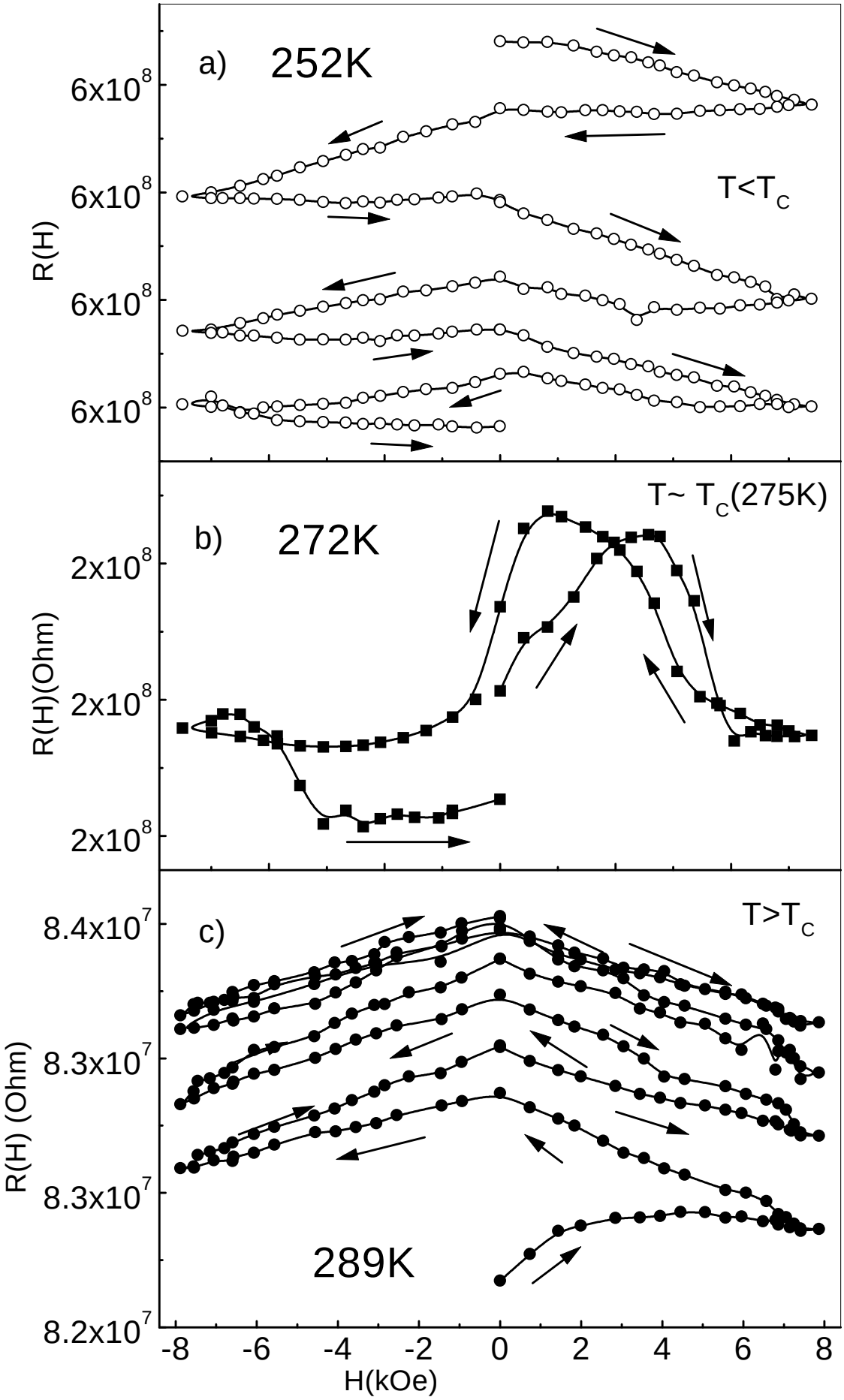

Fig.9 Magnetoresistance measured for more than one cyle of appled field ±8 Tesla.